

¹ Johan Hadi Wardoyo *² Mohammad Isa Irawan

Management of Steam Power Plant Operation Patterns by Using CPF Based Technology to Analyze Fuel Fluidization Characteristics in CFB Type Boiler



Abstract: - The need for electrical energy nationally continues to grow every year, the government has issued a national energy policy. Consideration that most of the 86.59% of the national coal reserves are low rank coal types, namely subbituminous and lignite with high sulfur content characteristics. Circulating Fluidized Bed (CFB) Boiler PLTU Labuhan Angin has fuel flexibility and lower emission. The flow in the Circulating Fluidized Bed (CFB) Boiler of PLTU Labuhan Angin is very non-linear with non-uniform constituent materials including bed particles, coal and limestone, so geldart classification must be carried out. In CFB boilers, generally have a gas-solid system characteristic, namely the recirculating loop of particles separated into the reactor from the carrier fluid in a process that must run efficiently. Under operating conditions, the particle flux reaches a high particle flux of 10-1000 kg/m² and a high superficial flux gas velocity of 2-212 m/s, so it is very possible to damage caused by wear. In order to maintain operational continuity, reliability and efficiency of power plants, improvement programs need to be carried out, one of which is related to carrying out Computational Particle Fluid Dynamic (CPF) simulation models on the Circulating Fluidized Bed (CFB) Boiler PLTU Labuhan Angin. In this thesis, an analysis of fluid flow characteristics and particle motion in the combustion chamber of PLTU Labuhan Angin 2 × 115 MW carried out using a Computational Particle Fluid Dynamic (CPF) simulation. The simulation carried out under normal operating conditions at the combustion chamber temperature which is close to the operating conditions at the design generating capacity (115 MW/unit). Computational Particle Fluid Dynamic (CPF) simulation modeling in the Circulating Fluidized Bed (CFB) Boiler PLTU Labuhan Angin is expected to be used to determine the velocity of gas and particle flow in the combustion chamber, temperature distribution in the combustion chamber, the dominant area of erosion potential as a baseline for geometry modification and recommendations. operation optimization programs.

Keywords: CFB Boiler, Fluidization, CPF, Geldart Classification, Erosion.

I. INTRODUCTION

PLTU Labuhan Angin uses a Circulator Fluidized Bed (CFB) boiler. CFB type boilers have advantages including fuel, high combustion efficiency, efficient sulfur absorption, low NO_x emissions, smaller furnace cross-section. In power plant operations, the boiler is a very important tool. The flow in the Circulator Fluidized Bed (CFB) Boiler PLTU Labuhan Angin is very non-linear with non-uniform constituent materials including bed particles, coal and limestone, so geldart classification must be carried out [1]. CFB boilers generally have the characteristics of a gas-solid system, namely a recirculation loop of particles that will be separated into the reactor from the carrier fluid in a process that must run efficiently [2]. Under operating conditions, particle fluidization reaches a high particle flux of 10-1000 kg/m² and a high superficial gas flux velocity of 2-212 m/s, so that the implementation of the co-firing program at the Labuhan Angin PLTU is very likely to cause damage caused by wear [3].

PLTU Labuhan Angin has been operating for 12 (twelve) years so it is possible that there is a potential decline in the performance of the operating pattern resulting in decreased efficiency. In order to support the co-firing program and maintain operational continuity, reliability and efficiency of power plants, it is necessary to carry out improvement programs, one of which is related to carrying out Computational Particle Fluid Dynamic (CPF) simulation modeling on the Circulating Fluidized Bed (CFB) Boiler of PLTU Labuhan Angin to determine the condition technically feasible operational patterns for coal firing and co-firing which include: gas and particle flow velocity in the combustion chamber, temperature distribution in the combustion chamber, dominant areas of potential erosion. This research is useful as a baseline for recommendations for programs to improve operational pattern management. It is hoped that after carrying out this research it can be used as an evaluation of the management of coal firing and co-firing operation patterns for PLTU Labuhan Angin.

¹ Interdisciplinary School of Management and Technology, Sepuluh Nopember Institute of Technology, Surabaya, Indonesia. 6032211115@student.its.ac.id

² Interdisciplinary School of Management and Technology, Sepuluh Nopember Institute of Technology, Surabaya, Indonesia. mii@its.ac.id

* Corresponding Author Email: 6032211115@student.its.ac.id

Copyright © JES 2024 on-line : journal.esrgroups.org

The selection of the Computational Particle Fluid Dynamic (CPFD) method is scientifically based on journals/applications in industry where it has been proven to be used to investigate optimal primary and secondary air flow in the maximum circulation rate of a fluidized bed [4]. Research using the CPFD model is also used to predict fuel and bed material fluidization flows with the aim of optimizing the process. Fuel fluidization that has been carried out using the CPFD method has carried out more in-depth research on the process of co-firing coal with biomass in the steam electric power plant (PLTU) industry which is of the Circulating Fluidized Bed (CFB) [5]. The Computational Particle Fluid Dynamic (CPFD) method is combined with another method, namely the Geldart classification method, which classifies particles into 4 groups, namely A, B, C, and this classification is plotted against the difference in particle density and the density of the fluid that is the fluidization medium [6]. Among the classifications of these particles, some are easy to fluidize and some are difficult. This Geldart classification can help in determining from the start whether a material is good for fluidization or not [7]. The combination of the Computational Particle Fluid Dynamic (CPFD) method with the Geldart classification method was carried out with the hope that the analysis results would be more comprehensive than previous research [8]. The objectives of the Computational Particle Fluid Dynamic (CPFD) research on the Circulating Fluidized Bed (CFB) Boiler PLTU Labuhan Angin are:

- Recommends a management program for coal firing and co-firing operations at PLTU Labuhan Angin to maintain operational continuity, performance and unit efficiency.
- Analyzing CFB boiler design, modeling and simulation to determine operational management using the CPFD CFB Boiler information technology system regarding fluid flow characteristics and the movement of material bed particles in the combustion chamber.
- Reliability Management by analyzing the flow velocity of gas and particles in the combustion chamber related to the temperature distribution in the combustion chamber and the dominant areas affected by erosion to reduce the rate of abrasion to increase the reliability of the Labuhan Angin PLTU.

II. RESEARCH METHODS

In this research, uses used for this analysis data:

1. Operational data collection methods
2. Quantitative approaches by comparing one variable with another
3. Determining the relationship between variables by sorting the problem into parts that can be measured or expressed in numerical form.

Operational data on Circulating Fluidized Bed (CFB) Boiler PLTU Labuhan Angin obtained becomes baseline data for analysis and evaluation using the Computational Particle Fluid Dynamic (CPFD) simulation modelling method.

A. Fluidization Conditions

Fluidization can be defined as a process that causes a granular solid to change into something similar to a fluid by allowing it to interact with a gas or liquid object [9]. The fluidization conditions of particles are classified into several conditions based on the superficial velocity of the gas used to fluidize the material. Pressure drop can be calculated using the equation:

$$\frac{\Delta P}{L} = 150 \frac{(1-\varepsilon)^2}{\varepsilon^3} \frac{\mu U}{(\phi d_p)^2} + 1.75 \frac{(1-\varepsilon)}{\varepsilon^3} \frac{(1-\varepsilon) \Delta P}{\phi d_p L} = 150 \frac{(1-\varepsilon)^2}{\varepsilon^3} \frac{\mu U}{(\phi d_p)^2} + 1.75 \frac{(1-\varepsilon)}{\varepsilon^3} \frac{(1-\varepsilon)}{\phi d_p} \tag{1}$$

The minimum fluidization velocity (Umf) value can be calculated using the equation:

$$F_D = \Delta P A = AL (1 - \varepsilon)(\rho_p - \rho_g) F_D = \Delta P A = AL (1 - \varepsilon)(\rho_p - \rho_g) \tag{2}$$

The incipient fluidized bed value can be calculated with the equation:

$$Re_{mf} = \frac{d_p U_{mf} \rho_p}{\mu} [CC_1^2 + C2Ar]0.5 - Cl Re_{mf} = \frac{d_p U_{mf} \rho_p}{\mu} [CC_1^2 + C2Ar]0.5 - Cl \tag{3}$$

Once the superficial air velocity is increased to a certain value exceeding Umf, the fluidization condition changes to a bubbling bed condition which can be predicted by solving the equation:

$$\frac{Um_b}{Um_f} = \frac{\mu^{0.523} \rho_g^{0.216} \exp(0.716F)}{d_p^{0.8} g^{0.934} (\rho_p - \rho_g)^{0.934}} \frac{Um_b}{Um_f} = \frac{\mu^{0.523} \rho_g^{0.216} \exp(0.716F)}{d_p^{0.8} g^{0.934} (\rho_p - \rho_g)^{0.934}} \tag{4}$$

A turbulent bed occurs when the superficial velocity exceeds the bubbling condition so that bubbles form and burst so quickly that the identity of the bubbling bed condition is no longer visible. One sign of the formation of turbulent conditions is the occurrence of fluctuations in pressure changes in the fluidization chamber. The amplitude of this pressure change fluctuation peaks at the fluidization velocity (u_k) and ends at the velocity (u_c) can be calculated using the equation:

$$Re_c = \frac{\mu_c d_p \rho_g}{\mu} = 0.936 Ar^{0.472} \quad Re_c = \frac{\mu_c d_p \rho_g}{\mu} = 0.936 Ar^{0.472} \tag{5}$$

$$Re_k = \frac{\mu_c d_p \rho_g}{\mu} = 1.46 Ar^{0.472} \quad Re_k = \frac{\mu_c d_p \rho_g}{\mu} = 1.46 Ar^{0.472} \quad (Ar < 10^4)10^4 \tag{6}$$

$$Re_k = \frac{\mu_c d_p \rho_g}{\mu} = 1.46 Ar^{0.472} \quad Re_k = \frac{\mu_c d_p \rho_g}{\mu} = 1.46 Ar^{0.472} \quad (Ar > 10^4)10^4 \tag{7}$$

This equation provides a lower limit for the occurrence of fast fluidization. Or in other words, fast fluidization will not occur before passing this speed.

$$U_{tr} = 1.45 \frac{\mu}{\rho_g d_p} Ar^{0.484} \quad U_{tr} = 1.45 \frac{\mu}{\rho_g d_p} Ar^{0.484} \quad (20 < Ar < 50000) \tag{8}$$

Table 1 Conditions that occur in several locations in the CFB boiler

Location	Condition
Bottom Furnace	Turbulent or bubbling
Upper Furnace	Fast fluidization
Cyclone	Swirl Flow
Return leg	Packed bed moving
Loop seal	Bubbling
Back pass	Pneumatic conveying

B. Geldart classification

Geldart (1972) classified particles into 4 groups, namely A, B, C, and D, and this classification was plotted against the difference in particle density and the density of the fluid that is the fluidization medium and the results can be seen in Figure 2 [10]. Group A particles have a diameter of 30 – 100 μm (ρ_p = 2500 kg/m³). These particles are well fluidized but can expand when the superficial gas velocity exceeds its minimum and goes into a bubbling state. Group B particles have a diameter of 100 – 500 μm (ρ_p = 2500 kg/m³). These particles are what most CFB boilers use because they fluidize easily and will reach the bubbling phase. Group C particles have a diameter smaller than 30 μm (ρ_p = 2500 kg/m³). These particles are difficult to channel. Group D particles have a diameter greater than 500 μm for conditions where ρ_p = 2500 kg/m³). A higher gas velocity is required to fluidize these particles.

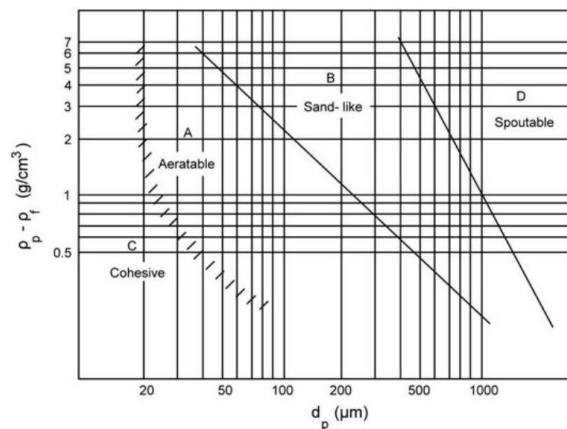


Fig.1. Geldart classification for granular solids

C. Computational Particle Fluid Dynamics (CPFD)

An approach using Multi-Phase Particle-in-Cell (MP-PIC) is used in this study where there are several governing equations to be solved (Andrews and O'Rourke, 1996; Snider, O'Rourke and Andrews, 1998; Snider, 2001) . The continuity and momentum equations can be written as follows:

$$\frac{\partial(\epsilon_g \rho_g)}{\partial t} + \nabla \cdot (\epsilon_g \rho_g u_g) = \frac{\partial(\epsilon_g \rho_g)}{\partial t} + \nabla \cdot (\epsilon_g \rho_g u_g) = 0 \tag{9}$$

$$\frac{\partial(\epsilon_g \rho_g)}{\partial t} + \nabla \cdot (\epsilon_g \rho_g u_g) = \frac{\partial(\epsilon_g \rho_g)}{\partial t} + \nabla \cdot (\epsilon_g \rho_g u_g) = -\nabla p + F + \epsilon_g \rho_g u_g + \nabla \cdot (\epsilon_g \tau_g) \nabla p + F + \epsilon_g \rho_g u_g + \nabla \cdot (\epsilon_g \tau_g) \tag{10}$$

The Wen-Yu drag model is used when dense solids can be calculated with the following equation:

$$D_p = C_d \frac{3}{8} \frac{\rho_p |u_g - u_p|}{r_p \rho_p} \tag{11}$$

The solids in the simulation can be predicted by solving the transport equation for the particle distribution function, f:

$$C_d W_{en} - Yu = \begin{cases} \frac{24}{Re} \text{ jika } Re < 0.2 \\ \frac{24}{Re} + 3.6 Re^{-0.313} \text{ jika } 0.2 < Re < 500 \\ 0.44 \text{ jika } Re > 500 \end{cases} \tag{12}$$

$$C_d W_{en} - Yu = 0.5 \left(\frac{180 \epsilon_p}{\epsilon_f Re} \right) \frac{\rho_p |u_g - u_p|}{r_p \rho_p} \tag{13}$$

$$\left\{ \begin{array}{l} C_d W_{en-yu} \text{ jika } \epsilon_p < 0.75 \epsilon_{cp} \\ (C_{d,Erqun} - C_d W_{en-yu}) \left(\frac{\epsilon_p - 0.75 \epsilon_{cp}}{0.85 \epsilon_p - 0.75 \epsilon_{cp}} \right) + C_d W_{en-yu} \text{ jika } 0.75 \epsilon_{cp} < \epsilon_p < 0.85 \epsilon_p \\ C_{d,Erqun} \text{ jika } \epsilon_p > 0.85 \epsilon_{cp} \end{array} \right\} \left\{ \begin{array}{l} C_d W_{en-yu} \text{ jika } \epsilon_p < 0.75 \epsilon_{cp} \\ (C_{d,Erqun} - C_d W_{en-yu}) \left(\frac{\epsilon_p - 0.75 \epsilon_{cp}}{0.85 \epsilon_p - 0.75 \epsilon_{cp}} \right) + C_d W_{en-yu} \text{ jika } 0.75 \epsilon_{cp} < \epsilon_p < 0.85 \epsilon_p \\ C_{d,Erqun} \text{ jika } \epsilon_p > 0.85 \epsilon_{cp} \end{array} \right. \tag{14}$$

$$a_p = \frac{d_{up}}{dt} \tag{16}$$

$$\frac{d_{up}}{dt} = D_p (u_g - u_p) - \frac{1}{\rho_p} \nabla p + g - \frac{1}{\epsilon_s \rho_p} \nabla \tau_g = 0 \tag{17}$$

MP-PIC utilizes different principles compared to conventional particle movement calculations that couple particle and fluid movements. In MP-PIC, these forces are predicted by calculating what is termed particle normal stress. This value is obtained by solving the following equation:

$$\tau_p = \frac{p_s \epsilon_s^\beta}{\max[(\epsilon_{cp} - \epsilon_p), \theta (1 - \epsilon_{cp})]} \tag{18}$$

D. Modeling Technology Information Systems

Operating System (Control System) programming is carried out on the CPFDF Boiler & Auxiliary modeling & simulation computer, so that analysis can be carried out to obtain Operation Patterns, Control Patterns that can be implemented into Actual Operations. Simulation, Setting & Tuning of Boiler & Auxiliary CFD Modeling & Simulation to obtain parameter data that can be applied to operations, to obtain efficient boilers and good performance.

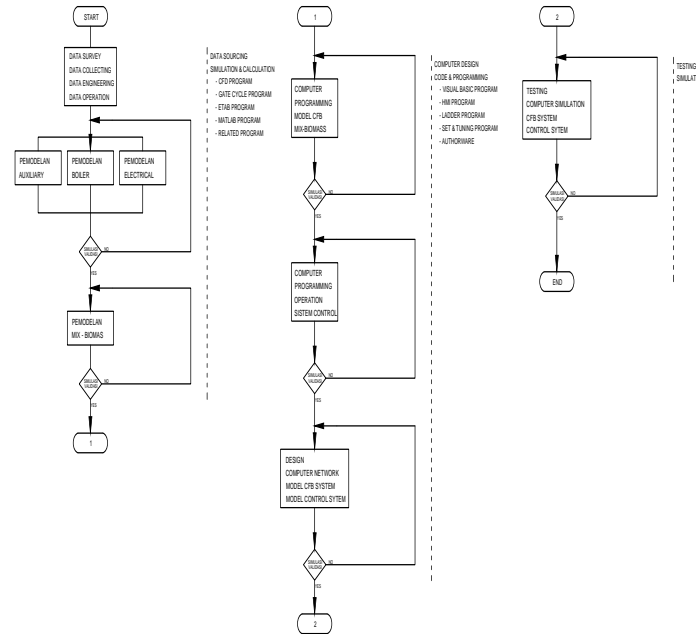


Fig.2. Simulation of CFB PLTU Labuhan Angin

E. Erosion

In the CFPD model, erosion modeling occurs when a mass hits a computational wall. Then termed impact, this will be recorded for each event and will be added up when the computing process is complete. The impact value is calculated using the equation:

$$I_p = w(\theta)m_p^a u_p^b I_p = w(\theta)m_p^a u_p^b \tag{19}$$

Calculate the volume of material lost due to erosion (Q) with the equation:

$$Q = \frac{m_p u_p^2}{p\psi K} \left(\sin 2\theta - \frac{6}{K} \sin^2 \theta \right) \tag{20}$$

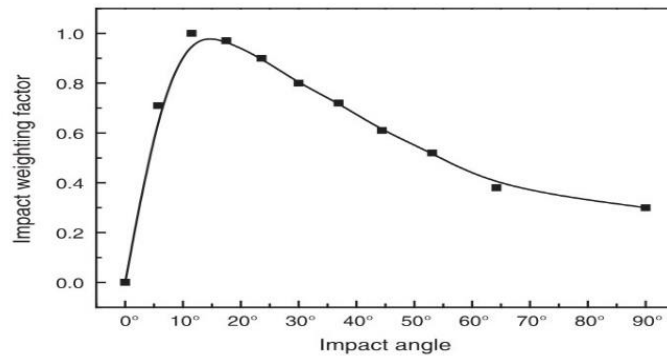


Fig .3. Weighting factor values at different angles

Figure 1 depicts the flow of the research process flow. The method used for this research analysis is as follows:

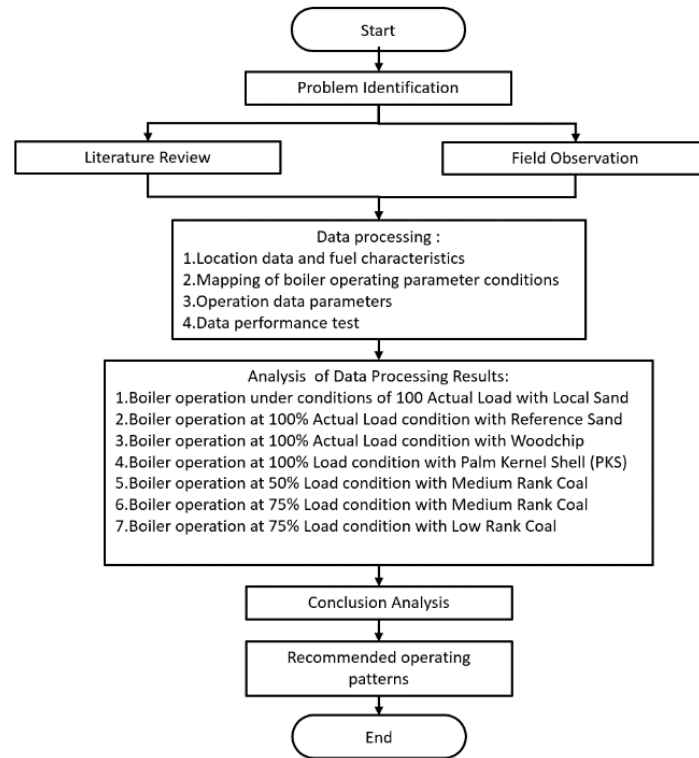


Fig.4. Research proses flow

III. RESULTS AND DISCUSSIONS

In this section, a discussion of the study of operational data on the Circulating Fluidized Bed (CFB) Boiler PLTU Labuhan Angin will be carried out using technology with the Computational Particle Fluid Dynamic (CPFD) simulation modeling method. Technical Recommendations for Optimum Operating Conditions of CFB Boilers that will be given include the condition of the coal used and the improvement of performance and targets that can be achieved. Modeling conditions are made with the following conditions:

1. Total number of all cells = 1,629,432
2. Total number of null cells = 458,171
3. Total number of natural cells = 1,171,261

A. Condition 100% Actual Load with Local Sand

The boiler simulation is performed transiently up to the 20th second. The data displayed includes particle temperature and volume impact throughout the boiler. At the 0th second, the particle temperature is still 1165 K but increases with the inclusion of coal, bottom flow, secondary air (SA), and primary air (PA). At the 2nd second, the particles move upward; at the 5th second, they enter the cyclone with increasing temperature. By the 10th second, all particles fill the boiler, with a hotspot visible at the loop seal. At the 15th second, the particle temperature drops throughout the boiler, including the seal loop. At the 20th second, the temperature distribution stabilizes with no hotspots.

The impact on the boiler increases with time. At the 0th second, there is no impact, but at the 2nd second, there is a significant impact at the bottom of the furnace. At the 5th second, the impact is evenly distributed at the bottom of the boiler, including the channel to the cyclone. At the 10th second, almost all boiler walls were impacted, except for the top side wall and loop seal. At the 15th second, a significant impact occurred on the upper sidewall, while the impact on the loop seal was relatively small. At the 20th second, all boiler parts were impacted, especially the cyclone and furnace walls. The fluid velocity pattern in the boiler is stable from the 2nd second to the 20th second, with the highest velocity in the cyclone inlet area. This causes particles to enter at high speed, causing high impact and erosion on the cyclone.

B. Condition 100% Load Condition with Reference Sand

Transient boiler simulation up to the 20th-second shows particle temperature data and isovolume impact on all parts of the boiler. At 100% load with reference sand, the 0th-second particle temperature remains 1165 K. The particle temperature increases With the input of coal, bottom flow, secondary water, and primary water. At the 2nd second, the particles move upward; at the 5th second, they enter the cyclone with an increase in temperature. At the 10th second, all particles fill the boiler with a hotspot at the loop seal. At the 15th second, the particle temperature drops throughout the boiler, including the seal loop. By the 20th second, the temperature distribution is steady with no hotspots, more even than the local sand.

The impact on the boiler increases with time. 0th second, no impact yet. 2nd second is a significant impact at the bottom of the furnace, especially the corner of the boiler wall. 5th second, they evenly distributed impact at the bottom of the boiler, including the channel to the cyclone. In the 10th second, almost all boiler walls were impacted except the top side wall and loop seal. 15th second, the impact is prominent on the upper side wall, while the loop seal impact is relatively small. In the 20th second, all boiler parts are impacted, especially the furnace wall and cyclone.

The fluid flow velocity in this simulation condition from the 2nd second to the 5th second is substantial in the cyclone area. When entering the 10th second to the 20th second, the fluid flow velocity in this area decreased. However, this also causes a very high impact and erosion on the cyclone wall. The reference sand causes a more significant impact on the boiler walls because it has a smaller size with the same air velocity. Therefore, it is best to use reference sand with a smaller airflow so fast beds do not occur.

C. Condition 100% Load Condition with Woodchip

The transient boiler simulation up to the 20th-second displays particle temperature and isovolume impact data throughout the boiler. At 100% load condition with woodchip, the particle temperature at the 0th second remains 1165 K. With the input of coal, bottom flow, secondary water, and primary water, the particle temperature increases. In the 2nd second, the particles move upward, and in the 5th second, they enter the cyclone with increasing temperature. At the 10th second, all particles fill the boiler with a hotspot at the loop seal. 15th second, particle temperature is evenly distributed throughout the boiler, including the seal loop. In the 20th second, there is a hotspot at the loop seal, but general particle temperature conditions are steady.

The impact on the boiler increases over time. 0th second, no impact yet. 2nd second is a significant impact at the bottom of the furnace, especially the corner of the boiler wall. 5th second, the impact is evenly distributed at the bottom of the boiler and the channel to the cyclone. In the 10th second, almost all boiler walls were impacted except the top sidewall and loop seal. 15th second, the upper side wall experienced a significant impact, while the loop seal impact was relatively small. At the 20th second, all boiler parts were impacted, especially the furnace wall.

The fluid flow velocity in this simulation condition is most significant in the cyclone section. From the 2nd second to the 5th second, the fluid velocity is very high at the inlet of the cyclone. When entering the 10th second to the 20th second, the fluid flow velocity at the lower cyclone inlet decreased. This causes a very high impact and erosion on the cyclone wall. In general, the conditions in the 100% load simulation using 5% woodchips do not show significant differences compared to the 100% load simulation without 5% woodchips in the particle temperature parameters and the impact experienced by the boiler walls. Therefore, the use of 5% woodchip as a co-firing fuel can be done.

D. Condition 100% Load Condition with Palm Kernel Shell

Transient boiler simulation up to the 20th-second displays particle temperature and isovolume impact data throughout the boiler. At 100% load condition with palm kernel shell, the particle temperature at the 0th second remains 1165 K. With the input of coal, bottom flow, secondary water, and primary water, the particle temperature increases. At the 2nd second, the particles move upward; at the 5th second, they enter the cyclone with increasing temperature. At the 10th second, all particles fill the boiler with a hotspot at the loop seal. 15th second, particle temperature is evenly distributed throughout the boiler, including the seal loop. In the 20th second, there is a hotspot at the loop seal, but general particle temperature conditions are steady.

The impact on the boiler increases over time. 0th second, no impact yet. 2nd second is a significant impact at the bottom of the furnace, especially the corner of the boiler wall. 5th second, the impact is evenly distributed at the bottom of the boiler and the channel to the cyclone. In the 10th second, almost all boiler walls were impacted, except the top side wall of the boiler and the loop seal wall. 15th second, the top side wall experienced a significant

impact, while the loop seal impact was relatively small. At the 20th second, all boiler parts were impacted, especially the furnace wall.

The fluid flow velocity in this simulation condition is most significant in the cyclone section. From the 2nd second to the 5th second, the fluid velocity is very high at the inlet of the cyclone. When entering the 10th second to the 20th second, the fluid flow velocity at the lower cyclone inlet decreased. This causes a very high impact and erosion on the cyclone wall. In general, the conditions in the 100% load simulation using palm kernel shell 5% do not show significant differences compared to the 100% load simulation without palm kernel shell 5% on the particle temperature parameters and the impact experienced by the boiler walls. Therefore, using palm kernel shell 5% as co-firing fuel is feasible.

E. Condition 50% Load Condition with Medium Rank Coal

Transient boiler simulation up to the 20th-second shows particle temperature and isovolume impact data in all parts of the boiler. In the 50% load condition with medium-rank coal, the particle temperature at the 0th second remains 1165 K. With the input of coal, bottom flow, secondary water, and primary water, the particle temperature increases. In the 2nd second, the particles move upward, and in the 5th second, they enter the cyclone with increasing temperature. At the 10th second, all particles fill the boiler with a hotspot at the loop seal. 15th second, particle temperature is evenly distributed throughout the boiler, including the seal loop. 20th second, hotspot at the loop seal, but particle temperature conditions are generally steady. The particle temperature distribution in the proper cyclone is more significant due to the higher coal flow rate in coal feed 2.

The impact on the boiler increases over time. 0th second, no impact yet. 2nd second is a significant impact at the bottom of the furnace, especially the corner of the boiler wall. In the 5th second, the impact is evenly distributed at the bottom of the boiler and the channel to the cyclone. In the 10th second, almost all boiler walls were impacted, except the top side wall of the boiler and the loop seal wall. 15th second, the top side wall experienced a significant impact, while the loop seal impact was relatively small. In the 20th second, all boiler parts were impacted, especially the furnace wall. The impact was generally smaller than the 100% load condition due to the lower air flow rate, resulting in smaller particle velocities.

The airflow velocity in this simulation condition has a pattern similar to that of the other simulation conditions. From the 2nd second to the 5th second, the maximum air velocity occurs at the cyclone inlet; after entering the 10th second to the 20th second, the airflow velocity at the cyclone inlet decreases, but the airflow velocity at the top of the cyclone inlet is still high. This causes high impact and erosion on the cyclone wall.

F. Condition 75% Condition Load with Medium Rank Coal

Transient boiler simulation up to the 20th-second displays particle temperature and isovolume impact data in all parts of the boiler. In the 75% load condition with medium-rank coal, the particle temperature at the 0th second remains 1165 K. With the input of coal, bottom flow, secondary water, and primary water, the particle temperature increases. In the 2nd second, the particles move upward, and in the 5th second, they enter the cyclone with increasing temperature. At the 10th second, all particles fill the boiler with a hotspot at the loop seal. 15th second, particle temperature is evenly distributed throughout the boiler, including the seal loop. In the 20th second, there is a hotspot at the loop seal, but general particle temperature conditions are steady.

The impact on the boiler increases over time. 0th second, no impact yet. 2nd second is a significant impact at the bottom of the furnace, especially the corner of the boiler wall. 5th second, the impact is evenly distributed at the bottom of the boiler and the channel to the cyclone. In the 10th second, almost all boiler walls were impacted, except the top side wall of the boiler and the loop seal wall. 15th second, the top side wall experienced a significant impact, while the loop seal impact was relatively small. At the 20th second, all boiler parts were impacted, especially the furnace wall.

In general, the impact experienced by the boiler in this simulation condition is smaller than with the 100% load condition because the air flow rate used is also smaller. This causes the particle velocity to be smaller so that the momentum generated when colliding with the wall becomes smaller.

G. Condition 75% Condition Load with Low-Rank Coal

Transient boiler simulation up to the 20th-second displays particle temperature and isovolume impact data in all parts of the boiler. In the 75% load condition with Low-Rank Coal, the particle temperature at the 0th second remains 1165 K. With the input of coal, bottom flow, secondary water, and primary water, the particle temperature

increases. In the 2nd second, the particles move upward, and in the 5th second, they enter the cyclone with increasing temperature. At the 10th second, all particles fill the boiler with a hotspot at the loop seal. 15th second, particle temperature is evenly distributed throughout the boiler, including the seal loop. In the 20th second, there is a hotspot at the loop seal, but general particle temperature conditions are steady.

The impact on the boiler increases over time. 0th second, no impact yet. 2nd second is a significant impact at the bottom of the furnace, especially the corner of the boiler wall. 5th second, the impact is evenly distributed at the bottom of the boiler and the channel to the cyclone. In the 10th second, almost all boiler walls were impacted, except the top side wall of the boiler and the loop seal wall. 15th second, the top side wall experienced a significant impact, while the loop seal impact was relatively small. At the 20th second, all boiler parts were impacted, especially the furnace wall.

The airflow velocity in this simulation condition has a pattern similar to that of the other simulation conditions. From the 2nd second to the 5th second, the maximum air velocity occurs at the cyclone inlet; after entering the 10th second to the 20th second, the airflow velocity at the cyclone inlet has decreased, but the airflow velocity at the top of the cyclone inlet is still high. This causes high impact and erosion on the cyclone wall. In general, the impact experienced by the boiler in this simulation condition is smaller than in the 100% load condition because the air flow rate used is also smaller. This causes the particle velocity to be smaller so that the momentum generated when colliding with the wall becomes smaller.

Calculation of Operating Costs and Co-Firing Capacity

This study addresses particle temperature and airflow patterns in the Labuhan Angin boiler and involves the calculation of comparative costs between 100% coal and co-firing conditions. The aim is to evaluate the possible benefits of co-firing, where the fuel is replaced with a composition of 95% coal, 5% woodchips, 95% coal, and 5% PKS. Table 2 provides data on the calorific value and price of each fuel used in the Labuhan Angin boiler.

DATA	MEDIUM RANK COAL	LOW RANK COAL	WOODCHIP	PKS
	MATANO	BARUNA POWER		
Kalor (kCal/kg)	4.729	4.152	4.132	4.264
Kalor (joule/kg)	19.786.136	17.371.968	17.288.288	17.840.576
Price/ton	921.382	858.255	750.000	750.000
Price/kg	921	858	750	750

The data shows that the prices of coal, woodchip, and PKS differ significantly. Table 3 shows the required heat requirement in each simulation condition.

No	Condition	Co-Firing Requirement (kg/s)	Coal Requirement (kg/s)	Co-Firing Requirement (kg/jam)	Coal Requirement (kg/jam)
1	100 MRC		19,653		70,750
2	100 Woodchip (5%)	0,983	18,670	3,538	67,213
3	100 PKS (5%)	0,983	18,670	3,538	67,213
4	50 MRC		12,131		43,670
5	75 MRC		15,028		54,100
6	75 LRC		15,028		54,100

From the table, the need for coal increases as the capacity of the power plant increases. For example, the coal requirement for 100% load capacity is 70750 kg/hour. Table 4 shows the results of calculating boiler operating costs in each condition

No	Total Calories (MW)	Total Cost (Rupiah/jam)	Kapasitas (MW)	Cost per MW (Rupiah)	Cost per kWh (Rupiah)
1	388,8525779	Rp65.187.756	115	Rp566.850	Rp567
2	386,3980950	Rp64.581.494	115	Rp561.578	Rp562
3	386,9407947	Rp64.581.494	115	Rp561.578	Rp562
4	240,0169099	Rp40.236.750	57,5	Rp699.770	Rp700
5	297,3416989	Rp49.846.752	86,25	Rp577.933	Rp578
6	297,3416989	Rp49.846.752	86,25	Rp577.933	Rp578

Data number 1 shows the amount of heat produced and the costs required for a 100% boiler load operation. Data numbers 2 and 3 show the heat produced and the costs incurred in 100% boiler load operation with co-firing 5% woodchip and PKS, respectively.

In terms of heat produced, the heat produced with co-firing is more minor when compared to full coal conditions. The difference in heat produced using 5% woodchip is 2.5 MW. However, the hourly cost required is also more minor. The cost saved by co-firing with 100% load capacity is about 1.5 million rupiah per hour.

IV. CONCLUSION

The conclusions that can be drawn from this CPFD software simulation are:

1. Management of coal firing and co-firing operational patterns:
 - Management of 100% coal firing operation pattern compared to 5% co-firing with a better heating value of 2.5 MW.
 - Management of the 5% biomass co-firing operation pattern can save operating costs of around 1.5 million rupiah per hour.
2. Operation Pattern Management:
 - Recommended :
 - Operating Pattern 100% load with Reference Sand
 - Operating Pattern 100% load with Woodchip
 - Operating Pattern 100% load with Palm Kernel Shell
 - Operation Pattern 50% load with Medium Rank Coal
 - Operation Pattern 75% load with Medium Rank Coal
 - Operation Pattern 75% load with Low Rank Coal
 - Not Recommended :
 - Operation Pattern 100% load with Local Sand
3. Reliability Management:
 - Operation Pattern 100% load with Local Sand by coating the wall and cyclone areas.
 - Operation Pattern 100% load with Reference Sand by controlling combustion air.
 - Operation Pattern 100% load with Woodchip by coating the wall area.
 - Operation Pattern 100% load with Palm Kernel Shell by coating the wall area.
 - Operation pattern 50% load with Medium Rank Coal can be carried out for long term operation.
 - Operation pattern 75% load with Medium Rank Coal can be carried out on a long term operation.
 - Operation pattern 75% load with Low Rank Coal can be carried out on a long term operation.

REFERENCES

- [1] Abbasi, A., Ege, P. E., & de Lasa, H. I. (2011). CPFD simulation of a fast fluidized bed steam coal gasifier feeding section. *Chemical Engineering Journal*, 174(1), 341–350. <https://doi.org/10.1016/j.cej.2011.07.085>
- [2] Basu, P. (2015). *Circulating fluidized bed boilers*. Springer International.
- [3] Chanel, P. G., & Doering, J. C. (2008). Assessment of spillway modeling using computational fluid dynamics. *Canadian Journal of Civil Engineering*, 35(12), 1481–1485. <https://doi.org/10.1139/L08-094>
- [4] Chen, C., Werther, J., Heinrich, S., Qi, H. Y., & Hartge, E. U. (2013). CPFD simulation of circulating fluidized bed risers. *Powder Technology*, 235, 238–247. <https://doi.org/10.1016/j.powtec.2012.10.014>
- [5] Fotoyat, F. (2014). Characterization of hydrodynamics and solids mixing in fluidized beds involving biomass. *Chemical Engineering*.
- [6] Jiang, Y., Qiu, G., & Wang, H. (2014). Modelling and experimental investigation of the full-loop gas-solid flow in a circulating fluidized bed with six cyclone separators. *Chemical Engineering Science*, 109, 85–97. <https://doi.org/10.1016/j.ces.2014.01.029>
- [7] Kokourine, A., & Adham, K. (2013). Three Dimensional Computational Modeling of Particulate Solids Segregation and Elutriation in a Commercial Scale Fluidized Bed Classifier. *The 14th International Conference on Fluidization - From Fundamentals to Products*, November.
- [8] Kraft, S., Kirnbauer, F., & Hofbauer, H. (2017). CPFD simulations of an industrial-sized dual fluidized bed steam gasification system of biomass with 8 MW fuel input. *Applied Energy*, 190(2017), 408–420. <https://doi.org/10.1016/j.apenergy.2016.12.113>
- [9] Li, J., Wang, W., Ge, W., & Yang, N. (2013). *From Multiscale Modeling to Meso-Science: A Chemical Engineering Perspective*. Springer.

- [10] Liang, Y., Zhang, Y., Li, T., & Lu, C. (2014). A critical validation study on CPFD model in simulating gas-solid bubbling fluidized beds. *Powder Technology*, 263, 121–134. <https://doi.org/10.1016/j.powtec.2014.05.003>
- [11] Liang, Y., Zhang, Y., & Lu, C. (2015). CPFD simulation on wear mechanisms in disk-donut FCC strippers. *Powder Technology*, 279, 269–281. <https://doi.org/10.1016/j.powtec.2015.04.012>
- [12] Qiu, G., Ye, J., & Wang, H. (2015). Investigation of gas-solids flow characteristics in a circulating fluidized bed with annular combustion chamber by pressure measurements and CPFD simulation. *Chemical Engineering Science*, 134, 433–447. <https://doi.org/10.1016/j.ces.2015.05.036>
- [13] Shah, S., Myöhänen, K., Kallio, S., & Hyppänen, T. (2015). CFD simulations of gas-solid flow in an industrial-scale circulating fluidized bed furnace using subgrid-scale drag models. *Particuology*, 18, 66–75. <https://doi.org/10.1016/j.partic.2014.05.008>
- [14] Thapa, R. K., Frohner, A., Tondi, G., Pfeifer, C., & Halvorsen, B. M. (2016). Circulating fluidized bed combustion reactor: Computational Particle Fluid Dynamic model validation and gas feed position optimization. *Computers and Chemical Engineering*, 92, 180–188.
- [15] Thapa, R. K., Pfeifer, C., & Halvorsen, B. M. (2014). International Journal Of Energy And Environment Modeling of reaction kinetics in bubbling fluidized bed biomass gasification reactor. *Journal Homepage: www.ijee.ieefoundation.org* ISSN, 5(1), 2076–2909. www.ijee.ieefoundation.org
- [16] Yagmur, L. (2016). Multi-criteria evaluation and priority analysis for localization equipment in a thermal power plant using the AHP (analytic hierarchy process). *Energy*, 94(2016), 476–482. <https://doi.org/10.1016/j.energy.2015.11.011>
- [17] Zhang, Y., & Wei, Q. (2017). CPFD simulation of bed-to-wall heat transfer in a gas-solids bubbling fluidized bed with an immersed vertical tube. *Chemical Engineering and Processing - Process Intensification*, 116, 17–28. <https://doi.org/10.1016/j.cep.2017.03.007>